Electronic Supplementary material

Perovskite-Mixed oxides Interactions to Modulate Overall Water Splitting Performance of $LaNiO_3$-Cu_xO/NiO Heterostructures

Nasrin Banu G, Rama Prakash M, Bernaurdshaw Neppolian*

Energy and environmental Remediation Laboratory, Department of Chemistry, Faculty of Engineering and Technology, SRM Institute of Science and Technology, Kattankulathur, Chennai, Tamil Nadu, 603203, India.

Table of contents

S1. Experimental Section

S1.1. Chemicals & Materials

Copper nitrate trihydrate ($Cu(NO_3)_2 \cdot 3H_2O$), nickel nitrate hexahydrate ($Ni(NO_3)_2 \cdot 6H_2O$), urea (CH_4N_2O), and ammonia (NH_3) were procured from SRL Chemicals. Lanthanum nitrate hexahydrate ($La(NO_3)_3 \cdot 6H_2O$), citric acid ($C_6H_8O_7$), commercial Pt/C (20 wt%), IrO_2, and Nafion (5.0 wt%) were purchased from Sigma-Aldrich. All chemicals were used without any further purification. Nickel foam with 99% porosity was obtained from Vitra Technologies. Deionized water was used wherever required, while ethanol was utilized for washing purposes.

S1.2. Pre-Treatment and Cleaning of Nickel Foam

Nickel foam pieces (1 × 1 cm^2) were first rinsed in dilute HCl to remove surface impurities and oxide layers. They were thoroughly washed in a cleaning solution comprising ethanol, acetone, and D.I. water in an 8:8:2 volume ratio. After washing, the nickel foam samples were dried overnight at 60°C to ensure complete removal of any residual moisture.

S1.3. Preparation of Pt-C/NF and IrO_2/NF

2 mg of 20 wt% commercial Pt/C was dispersed in 1 mL of a water-Nafion-ethanol mixture (volume ratio 6:3:1) and sonicated for 20 minutes to obtain a uniform catalyst ink. Subsequently, 20 μL of the homogenized ink was drop-cast onto a 1 × 1 cm^2 nickel foam substrate and dried under ambient conditions for 4 hours. The IrO_2 electrode was prepared in a similar manner and denoted as IrO_2/NF.

S1.4. Physico-chemical Characterizations

The phase composition of the synthesized composites was analyzed by X-ray diffraction (XRD, BRUKER, Cu Kα, λ = 1.5418 Å). Surface chemical states were examined using X-ray

photoelectron spectroscopy (XPS, Thermo Scientific, K-Alpha). The morphology and microstructure were characterized by field emission scanning electron microscopy (FE-SEM, Quanta 200) and transmission electron microscopy (TEM, JEOL, 200 kV). The charge characteristics of the materials were determined through zeta potential analysis (Malvern, U.K.). Functional group identification was carried out using Fourier Transform Infrared Spectroscopy (FTIR, Bruker Tensor 27). The evolved gases (H_2 and O_2) during electrochemical testing were quantitatively analyzed using gas chromatography (AGILENT, 7890B).

S1.5. Electrochemical measurements

The HER and OER tests were performed in 1 M KOH solution utilizing a three-electrode setup by an electrochemical station, Metrohm Multi Autolab M204, wherein Hg/HgO (1 M KOH) and graphite rod were employed as the reference and counter electrode, respectively. The nickel foam was cleaned, dried and modified with the synthesized Cu-Ni-O/$LaNiO_3$ as follows. Cu-Ni-O/$LaNiO_3$ in the ratio of 9:1 was homogenized with 1mL solution of water-nafion-ethanol (taken in 6:3:1 volume ratio) by sonicating for 15 min. About 20 µL of the homogenized ink was casted on 1 x 1 cm^2 nickel foam and dried at ambient conditions for 10 h. These modified electrodes were used as working electrodes during all electrochemical measurements and characterizations which were done at ambient conditions. All potentials were converted to the reversible hydrogen electrode (RHE) scale. The HER and OER performance were analyzed using linear sweep voltammetry (LSV) at a scan rate of 5 mV s^{-1} from -0.5 to -1.5 V and 0.5 to 2.0 V vs. Hg/HgO. The Electrochemical Impedance Spectroscopy (EIS) test was conducted from 1 kHz to 1 mHz to investigate the charge transfer ability of the as-prepared catalyst. The stability test was performed using chronoamperometry method. The electrochemical active surface area (ECSA) was studied using cyclic voltammetry with scan rate of 20 to 100 mV s^{-1} at non faradaic region. Stability test was performed using chronoamperometry in 1 M KOH.

S1.6. Two Electrode Set-up Details

The overall water-splitting performance was evaluated in a two-electrode configuration using Cu-Ni-O/$LaNiO_3$/NF as both the cathode and anode. The electrochemical measurements were conducted in 1 M KOH electrolyte (20 mL) under ambient conditions. Linear sweep voltammetry (LSV) was performed in the potential range of 1.0-2.5 V at a scan rate of 5 mV s^{-1} to assess the catalytic activity. The long-term stability of the catalyst was examined by chronoamperometric measurements in the same two-electrode setup.

S2. Synthesis Procedure

S2.1. Synthesis of Cu_xO/NiO (Cu-Ni-O)

Cu_xO/NiO was synthesized via a hydrothermal method. Copper nitrate trihydrate (1 mmol), Nickel nitrate hexahydrate (2 mmol) and urea (10 mmol) were dissolved in 40 mL of D.I. water. The resulting solution was stirred for 30 min to ensure complete dissolution and homogeneity. The solution was then transferred to a Teflon-lined stainless-steel autoclave and heated at 180°C for 10 h to promote controlled crystal growth. After cooling to room temperature, the precipitate was collected, thoroughly washed with D.I. water and ethanol and then dried for 12 h. The material was subsequently calcined at 250°C for 2 h to decompose the hydroxides into the corresponding Cu-Ni-O.

S2.2. Synthesis of Lanthanum Nickel Oxide - $LaNiO_3$

Lanthanum Nickelate was synthesized via a sol-gel method. Lanthanum nitrate hexahydrate (1 mmol), Nickel nitrate hexahydrate (2 mmol) and citric acid (4 mmol) were dissolved in 20 mL of D.I. water. The pH of the solution was adjusted to 7 using ammonia to promote complexation. The solution was then heated to 80°C for 10 h to form a homogeneous gel. The gel was dried overnight at 80°C, followed by calcination at 550°C for 2 h to decompose hydroxides into the Lanthanum-nickel oxide

S2.3. Synthesis of $Cu_xO/NiO/LaNiO_3$ - (Cu-Ni-O/$LaNiO_3$)

The Cu-Ni-O/$LaNiO_3$ composite with a weight ratio of 9:1 was prepared via simple physical mixing. Pre-synthesized Cu_xO/NiO and $LaNiO_3$ powders were accurately weighed and thoroughly ground together for 30 min to ensure uniform mixing and intimate contact between the particles. Zeta potential measurements in Fig. S2 indicates that both Cu-Ni-O (-12.5 mV) and $LaNiO_3$ (-30.1 mV) are negatively charged in aqueous dispersions, which lead to electrostatic repulsion. While this repulsion would not favour spontaneous aggregation in

solution, the mechanical grinding effectively overcomes it, resulting in a homogeneous composite with uniform distribution of $LaNiO_3$ within the Cu-Ni-O matrix. The negative surface charge also helps prevent uncontrolled agglomeration, promoting a well-dispersed composite suitable for subsequent electrochemical studies.

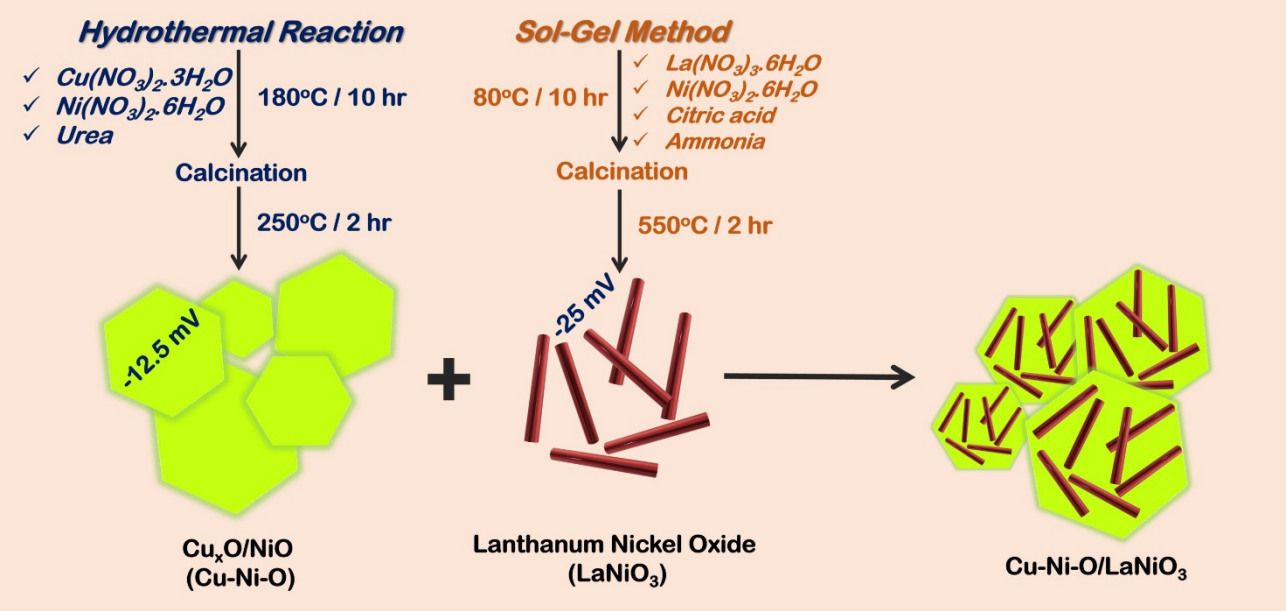

Fig. S1. Schematic representation of Cu_xO/NiO (Cu-Ni-O), Lanthanum Nickelate ($LaNiO_3$) and Cu-Ni-O/$LaNiO_3$ composite.

S2.4. Zeta Potential Measurements

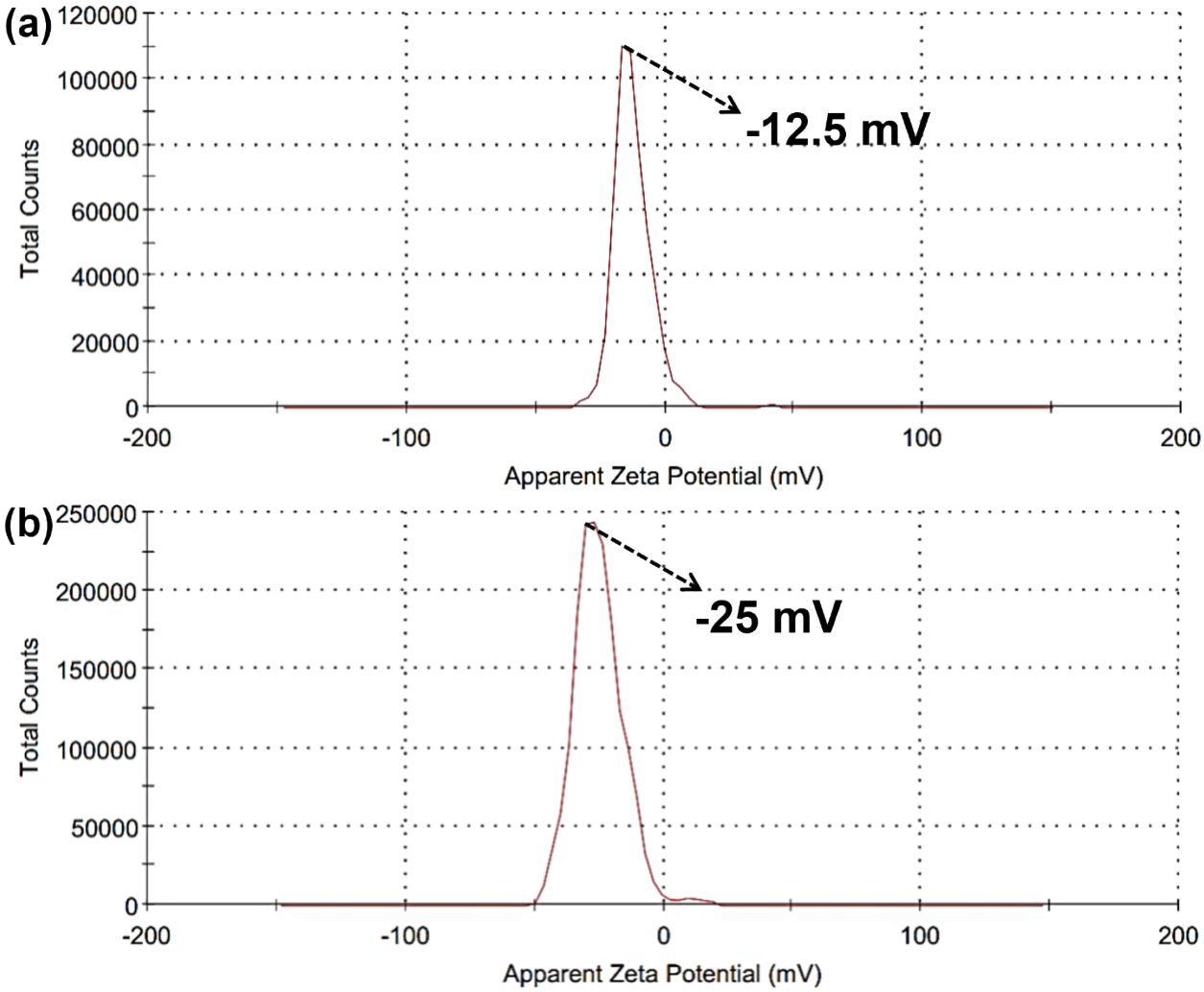

Fig. S2. Zeta potential measurements of (a) Cu-Ni-O and (b) $LaNiO_3$.

S3. Supporting figures and tables

S3.1. XRD Pattern

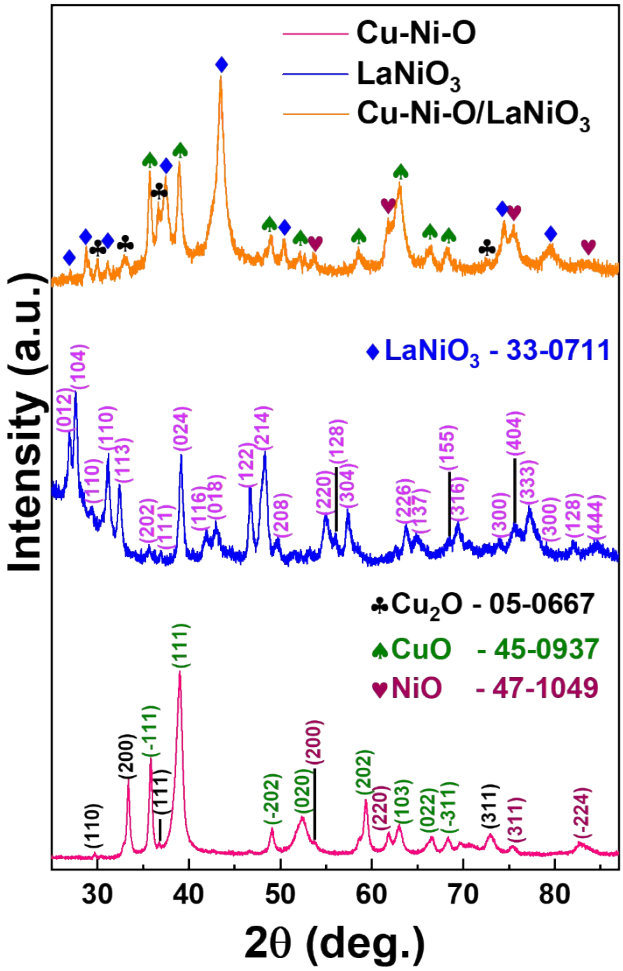

Fig. S3. XRD Patterns of Cu-Ni-O, $LaNiO_3$ and Cu-Ni-O/$LaNiO_3$.

S3.2. FTIR Spectrum

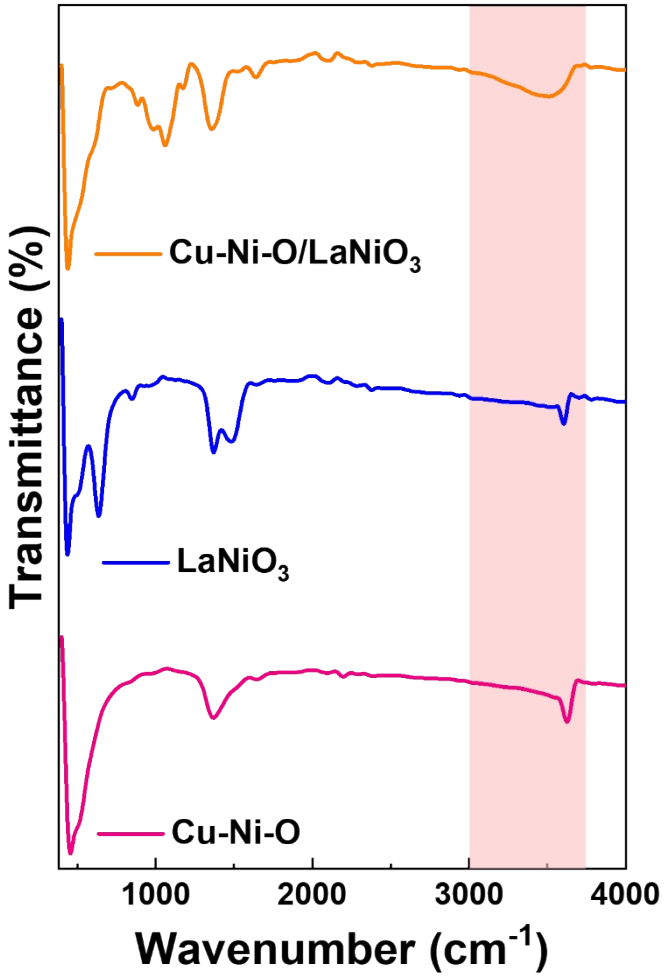

Fig. S4. FTIR Spectrum of Cu-Ni-O, $LaNiO_3$ and Cu-Ni-O/$LaNiO_3$.

S3.3. XPS Analysis

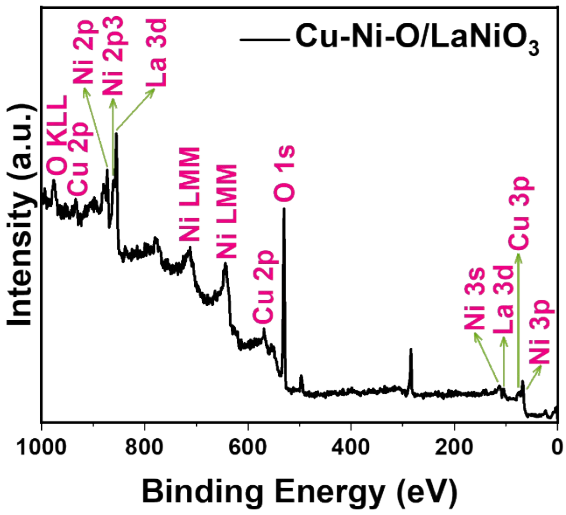

Fig. S5. XPS Survey Spectrum of Cu-Ni-O/$LaNiO_3$.

S4. Electrochemical studies

S4.1. Electrochemical Impedance Spectroscopy (EIS) Studies

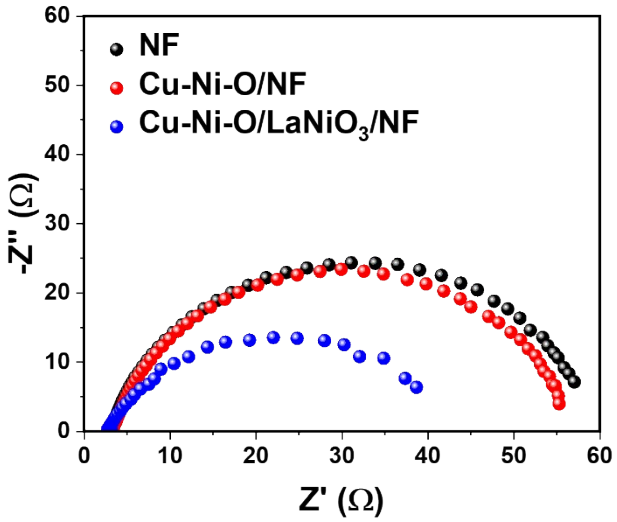

Materials	R_s (Ω/cm^2)	R_{ct} (Ω/cm^2)
NF	**3.308**	**55.790**
Cu-Ni-O/NF	**3.486**	**52.139**
Cu-Ni-O/$LaNiO_3$/NF	**2.953**	**38.756**

Fig. S6. Nyquist plot of NF, Cu-Ni-O & Cu-Ni-O/$LaNiO_3$ for HER test.

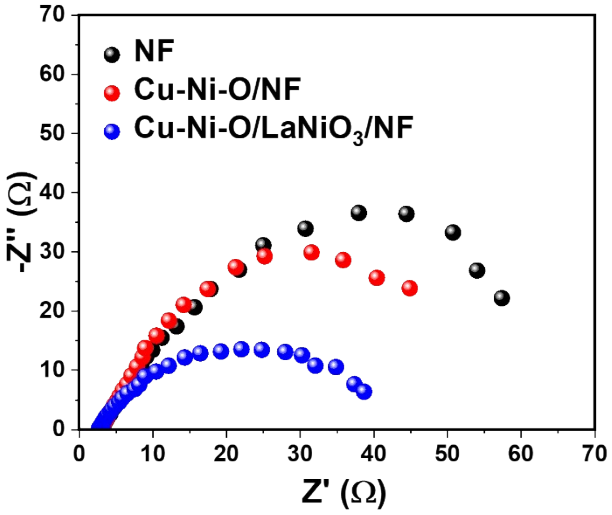

Materials	R_s (Ω/cm^2)	R_{ct} (Ω/cm^2)
NF	**3.796**	**60.904**
Cu-Ni-O/NF	**3.381**	**53.839**
Cu-Ni-O/$LaNiO_3$/NF	**3.174**	**38.826**

Fig. S7. Nyquist plot of NF, Cu-Ni-O & Cu-Ni-O/$LaNiO_3$ for OER test.

S4.2. Calculation of Double Layer Capacitance (C_{dl})

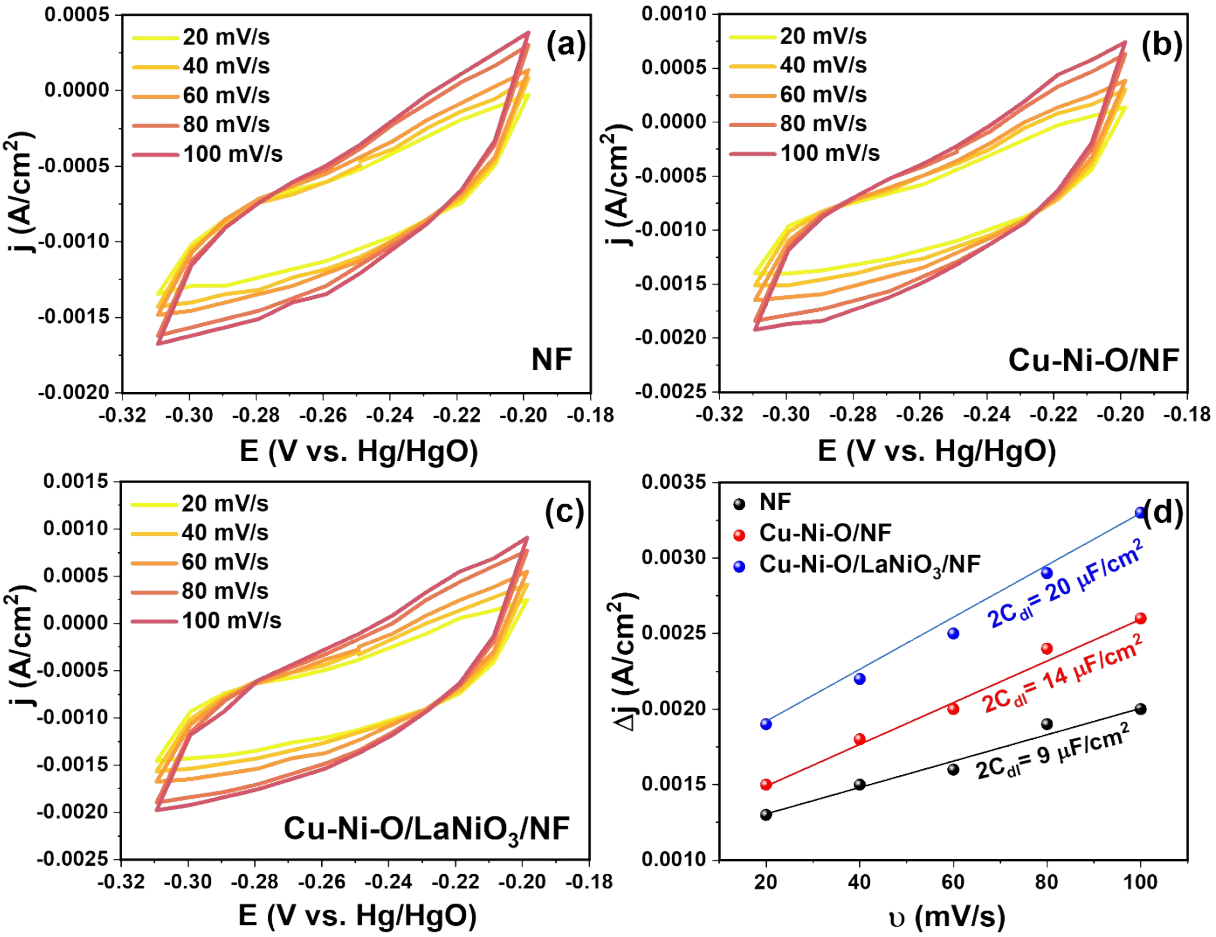

Fig. S7. Cyclic voltammograms of (a) NF, (b) Cu-Ni-O/NF and (c) Cu-Ni-O/$LaNiO_3$/NF with various scan rates (20, 40, 60, 80, 100 mV/s) and (d) plot of change in current density vs. Scan rate.

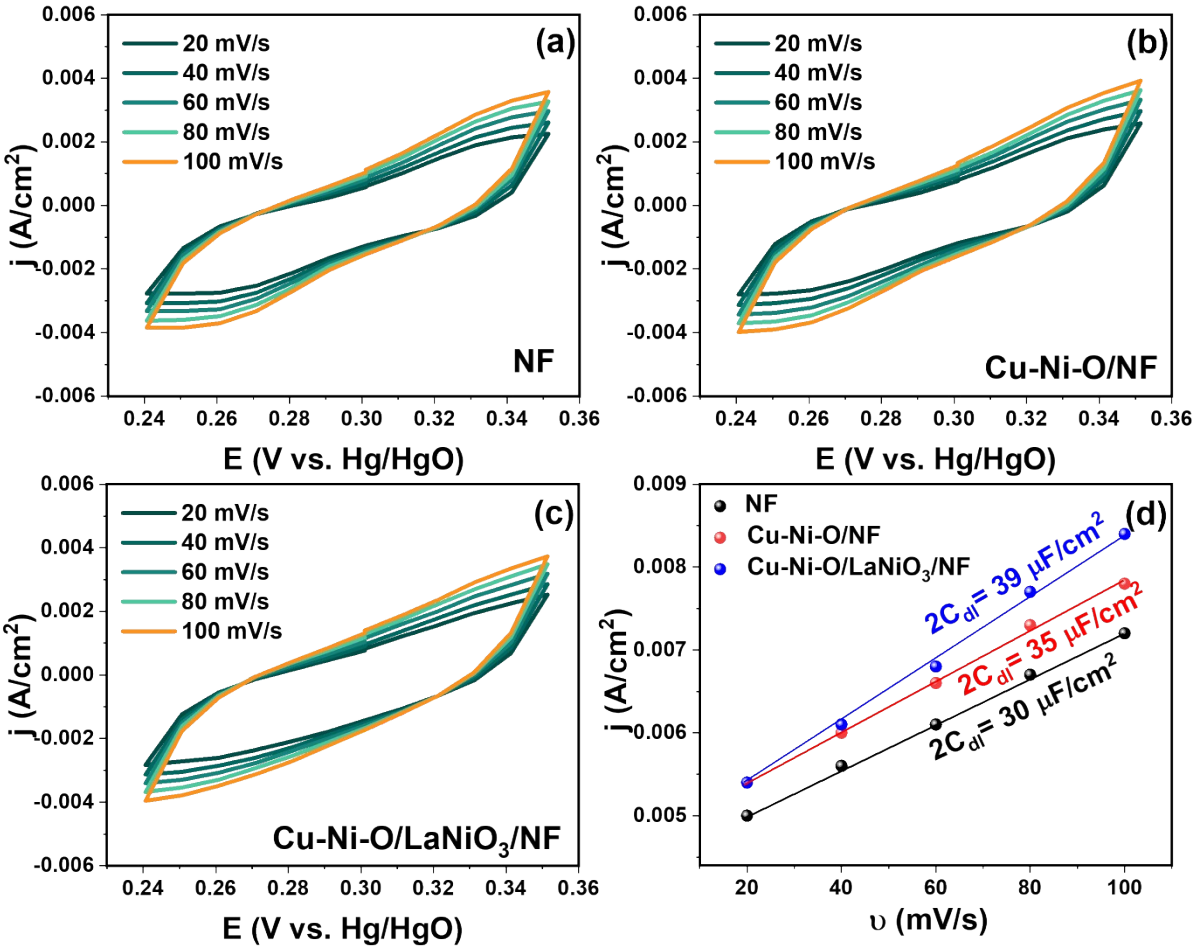

Fig. S8. Cyclic voltammograms of (a) NF, (b) Cu-Ni-O/NF and (c) Cu-Ni-O/$LaNiO_3$/NF with various scan rates (20, 40, 60, 80, 100 mV/s) and (d) plot of change in current density vs. Scan rate.

S5. Comparison Studies

S5.1. Comparison Study for HER Activity

Catalysts	Overpotential @10mA/cm^2	Reference
$CuS/CuCo_2O_4$	135	[1]
$CuCo_2S_4$	142	[2]
Copper Ferrite	241	[3]
$NiCo_2O_4@MoS_2$	180	[4]
$NiCoFeO_4$	167	[5]
Cu-Ni-O/$LaNiO_3$/NF	98	This work

Table S3. Comparison of HER activity of Cu-Ni-O/$LaNiO_3$/NF with other recently reported similar electrocatalysts

S5.2. Comparison Study for OER Activity

Catalysts	Overpotential @10mA/cm^2	Reference
$NiCo_2O_4$@MoS_2	355	[4]
$NiCoFeO_4$	450	[5]
rGO/NMC	320	[6]
Fe_3O_4/NF	310	[7]
$ZnNiFeO_4$	311	[8]
Cu-Ni-O/$LaNiO_3$/NF	290	This work

Table S4. Comparison of OER activity of Cu-Ni-O/$LaNiO_3$/NF with other recently reported similar electrocatalysts

S5.2. Comparison Study for OWS Activity

Catalysts	Cell Voltage @10mA/cm^2	Reference
$CuCo_2S_4$	1.53	[2]
$NiCo_2O_4$/NiO/CoF_2@mC	1.56	[9]
$NiCo_2O_4$@MoS_2	1.72	[4]
$NiCoFeO_4$	1.83	[5]
NCO-NSs	1.65	[10]
Cu-Ni-O/$LaNiO_3$/NF	1.5	This work

Table S5. Comparison of OWS activity of Cu-Ni-O/$LaNiO_3$/NF with other recently reported similar electrocatalysts

S6. Post stability analysis

S6.1. Morphological Analysis

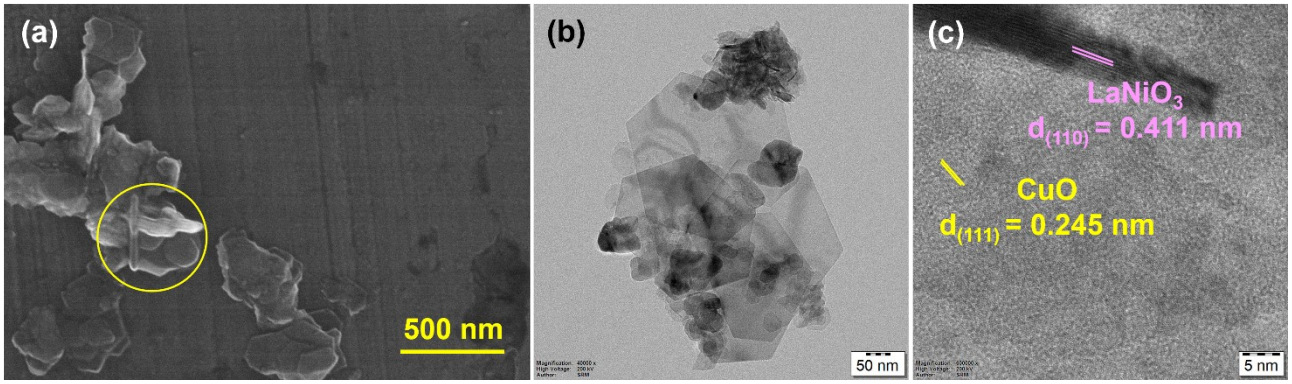

Fig. S9. (a) SEM image, (b) TEM image and (c) HRTEM image of Cu-Ni-O/$LaNiO_3$/NF after HER test.

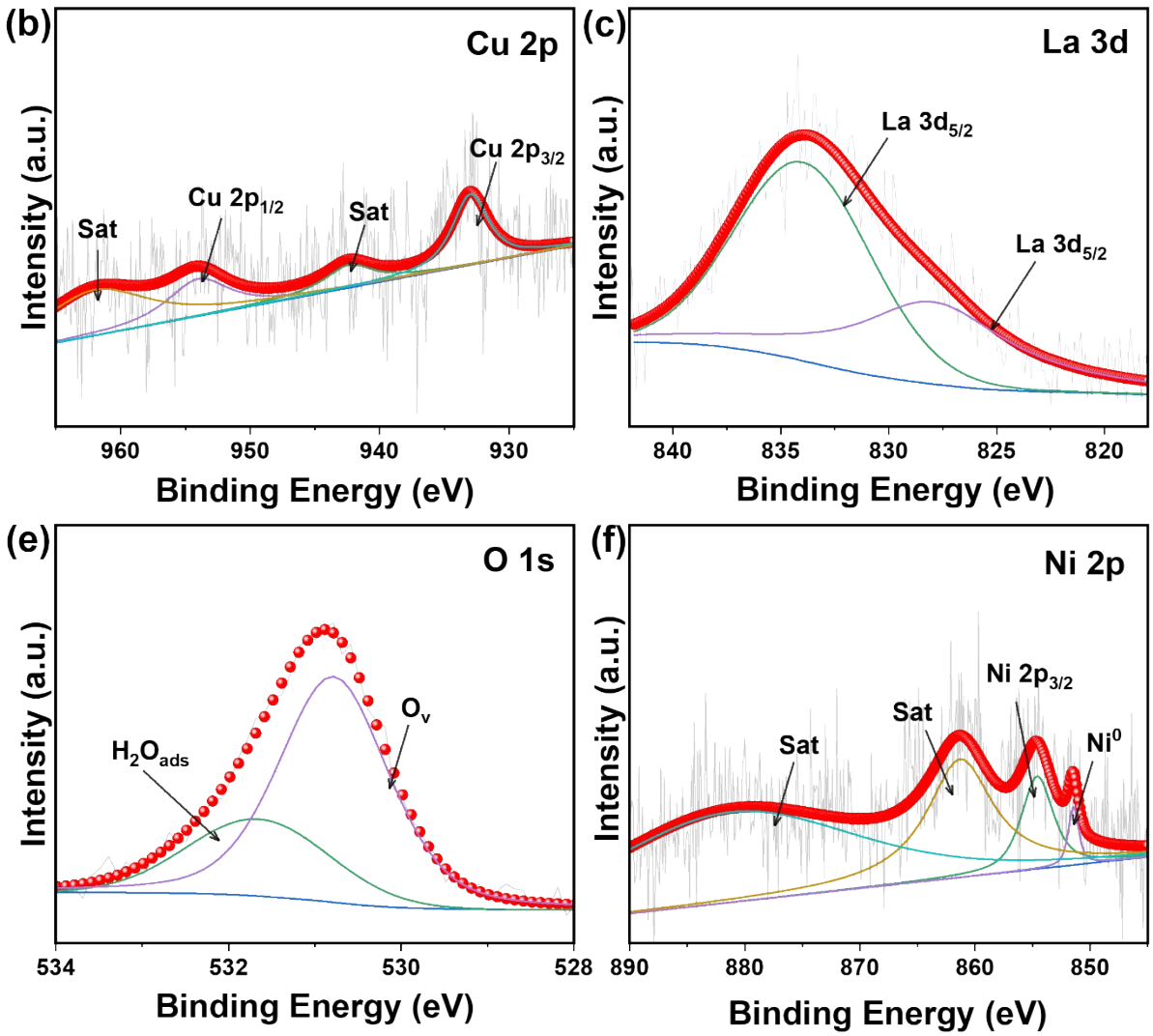

S6.2. XPS Analysis

Fig. S10. XPS spectrum of (a) Cu 2p, (b) La 3d, (c) O 1s and (d) Ni 2p of Cu-Ni-O/$LaNiO_3$/NF after HER test.

S7. References

[S1] M. M. Khan, Syed, H. Shah, Muhammad Najam-ul-Haq, N. H. Alotaibi, S. Mohammad, I. Zada, Muhammad Naeem Ashiq and S. I. Allakhverdiev, Journal of Electroanalytical Chemistry, 2024, 967, 118450–118450.

[S2] X. Du, Y. Ding, H. Su and X. Zhang, International Journal of Hydrogen Energy, 2020, 45, 12012–12025.

[S3] J. Tan, S. Xu, H. Zhang, H. Cao and G. Zheng, Electrochimica Acta, 2021, 381, 138199.

[S4] J. Li, D. Chu, D. R. Baker, H. Dong, R. Jiang and D. T. Tran, Chemistry of Materials, 2019, 31, 7590–7600.

[S5] S. Benny, W. Galeb, S. Ezhilarasi, J. D. Rodney, N.K. Udayashankar, M. D. Raja, J. Madhavan and S. Arulmozhi, Inorganic Chemistry Communications, 2025, 174, 114044–114044.

[S6] R. Miao, J. He, S. Sahoo, Z. Luo, W. Zhong, S.-Y. Chen, C. Guild, T. Jafari, B. Dutta, S. A. Cetegen, M. Wang, S. P. Alpay and S. L. Suib, "ACS Catal, 2017, 7, 819–832.

[S7] A. A. Pawar, H. A. Bandal and H. Kim, Journal of Alloys and Compounds, 2021, 863, 158742.

[S8] N. A. Khan, G. Rahman, S. Y. Chae, N. Yoon, A. ul H. A. Shah and S. A. Mian, ACS Applied Energy Materials, 2024, 7, 4960–4974.

[S9] S. Wu, J. Liu, B. Cui, Y. Li, Y. Liu, B. Hu, L. He, M. Wang, Z. Zhang, K. Tian and Y. Song, Electrochim. Acta, 2019, 299, 231–244.

[S10] L. Tao, Y. Li, M. Li, G. Gao, X. Xiao, M. Wang, X. Jiang, Xiaowei Lv, Q. Li, S. Zhang, Z. Zhao, C. Zhao and Y. Shen, The Journal of Physical Chemistry C, 2017, 121, 25888–25897.